Hindawi
Mobile Information Systems
Volume 2022, Article ID 3777613, 8 pages
https://doi.org/10.1155/2022/3777613

Research Article

Analyzing Welding Performance of Metal Using Artificial Neural Network

Xiaojun Wu

Institute of Automobile Engineering, Chongqing Industry Polytechnic College, Chongqing 401120, China

Correspondence should be addressed to Xiaojun Wu; wuxj@cqipc.edu.cn

Received 18 April 2022; Revised 21 May 2022; Accepted 9 June 2022; Published 23 June 2022

Academic Editor: Abid Yahya

In recent years, the speed of modernization construction in China has been exponentially growing. The trend of high parameters, large capacity, and large-scale development of the welding structure has been promoted. It needs higher requirements on the type and quality of the welding materials. Most of the welding materials are imported to China. The main reason is that China still follows the traditional design method. The quality of the welding materials is also low. The design of metal welding materials involves many factors and properties. There is no fixed-function relationship between the properties and components of the welding materials. This makes it difficult to design metal welding materials. The emergence of neural network algorithms provides a new way to analyze the weldability of metal materials. In this paper, BP (backpropagation) network is used to analyze the welding performance of metals. The tensile test of welded joints is carried out through training test samples. The results show that the tensile strength and yield strength of metal materials are about 500 MPa (megapascals) and 400 MPa, respectively. For further analysis of the influence of welding current, electrode pressure, and power-on time on the tensile and shear strength of metal materials, a shear test and tension test were used. With the increase of welding current, the shear strength of spot welding continuously increased. When the welding current was 10,000A (Ampere), the shear strength decreased rapidly from 24.25 MPa to 18.84 MPa. After prolonging the welding time, at first, both tensile strength and shear strength increase and then decrease. When the welding pressure increases from 32psi to 48psi, the tensile strength increases from 16.47 MPa to 24.52 MPa and then decreases continuously to 17.26 MPa, whereas the shear strength decreases first and then increases.

1. Introduction

In today's production, ARC welding technologies play a critical role. Despite the ubiquitous use of arc welding to combine metals, the human welder still needs extensive skills and expertise to regulate most welding operations. Total welding automation has yet to be realized, owing to a lack of understanding and quantification of the physics that govern the performance of any welding process. In terms of metal material welding, it is a process of sculpting and joining metals. During the welding process, the material is produced by melting or not the workpiece to the solder but they are used to join to the weld. This process also requires a certain amount of pressure to be applied to ensure the joining of the solder [1].

The total size of the molten weld bead is one of the most important features of the weld itself. Certain geometric characteristics, such as crown width, root width, and penetration, are only a few of the criteria that should be monitored during the procedure. Other characteristics that may be measured to a lesser extent, such as overall weld look and the absence of discontinuities, should be managed in the end. In order to ensure the welding effect, factors such as the welding process, the hardness of the welding material, and the surrounding environment are analyzed. However, at the same time, the spot welding strength will be affected by the change in the welding electrode voltage, current, and power. To solve this problem, a neural network algorithm is used to analyze the welding performance of metal materials. Artificial neural network (ANN) develops rapidly and is widely used in various fields. In this paper, ANN is used to analyze the welding performance of metal materials. The tensile test is used to judge the tensile strength and yield strength of

metal welding wires. Data collected during the welding process are analyzed by ANN to judge the quality of welded joints.

The main innovations in this research process are as follows:

(i) First, the basic concepts of the artificial neural network algorithm are explained, then the BP network model is established, and the calculation process and basic structure of the algorithm are described in detail.

(ii) Based on the artificial neural network (ANN) to analyze the welding chemical composition of metal materials, through collecting learning samples and processing sample data, the tensile test of metal materials' welded joints is completed based on statistical data. The test results show that the tensile strength and yield strength of welded joints filled with the same composition of wire are 500 MPa and 400 MPa, respectively.

(iii) Furthermore, digitized weld bead profiles derived from a laser-based bead surface scanner now in use at NASA were analyzed using artificial neural networks. The networks gave a better way of determining the placement of important bead properties including the crown, undercuts, and edges automatically.

The rest of the research paper is structured as follows; Section 2 explains the related work. It is being followed by Section 3 which explains artificial neural network algorithms. Similarly, Section 4 elaborates an analysis of the welding performance of metal materials based on a neural network. Finally, welding performance result analysis and concluding remarks are described in Sections 5 and 6, respectively.

2. Related Work

Presently, the artificial neural network has been widely used in the field of welding. Among these, the most common applications are in the design of welding parameters, prediction of weld joint performance, control of spot welding quality, prediction of HAZ performance, and tracking of the weld seam. The results are also remarkable [2]. Some UK welding research institutes and units have introduced artificial neural network technology into the welding process. Plonis experts study the neural network technical support required for welding engineering and formulate corresponding neural network software packages for different production condition manufacturers. Mahmud's scholars point out that weldability is used to indicate whether steel can adapt to the welding processing to produce weld joint characteristics with ideal performance and no defects. These include weld joint mechanics and resistance of steel to weld cracks [3]. Tagiltsev et al. welded T-type joints using low-temperature phase-change welding wire. The results show that the angular distortion of this low-temperature phase-change welding joint is smaller than the normal welding wire joints [4]. Sahaet al. have studied the distribution of residual stress in welds and proposed that ideal residual stress distribution can be found in welded structures when the initial temperature of wire phase transformation is maintained at 200 C. Govindan et al. explore AZ31 (alloy) B magnesium alloy sheet by TIG (tungsten inert gas) welding. He focused on the analysis of the factors leading to defects in AZ31B (alloy) magnesium alloy TIG welded joints and summarized some measures to deal with the defects [5]. Chen et al. deeply analyzed the susceptibility of solidification cracks in AZ31 magnesium alloy weld by TIG welding. Using AC/DC TIG welder as the welding equipment, the susceptibility analysis of cracks is affected by pulse frequency [6]. Ren et al. found two main factors the wire feed speed and heat input during MIG (metal inert gas) welding of magnesium alloy affecting the macro-surface forming of the weld [7]. Xu K W et al. explore various factors that affect the weld performance of AZ31 magnesium alloy plate welded by MIG. In this experiment, AZ31 is selected as the welding base material, and MIG is welded by a DC power source. AZ61 (alloy) is filled with metal. The welding speed is 3M per minute. The results show that the MIG welding speed and current have a direct impact on the macro-surface formation of AZ31 magnesium alloy sheet weld. The tensile strength of the welded joint is about 98% compared with the base metal. Feng et al. studied the effect of surface treatment on the performance of welded joints of AZ31 B magnesium alloy by ultrasonic welding. A large number of surface treatment comparisons were used during this experiment. Mg(OH) film was formed on the surface of AZ31B magnesium alloy after alkaline washing. The peeling occurred as a result of the welding procedure. It caused the structure and functioning of the joints to deteriorate. The $Mg(OH)_2$ film layer can be cleaned with a mixed acid solution to enhance the welding effect [8]. Chen et al. found that analysis of mechanical properties of friction stir welded joint of AZ31 magnesium alloy shows that the tensile strength of friction stir welded joint is 90% of the base material [9].

3. Artificial Neural Network Algorithms

In this section, first, we will discuss the artificial neural networks and its main characteristics. After that, BP neural model is explained along with a diagram. Finally, BP neural network learning algorithm is briefly explained. The explanation is as follows.

3.1. Artificial Neural Network. The artificial neural network has a sample processing unit. It collectively completes the work. Its storage mode and information transmission mode are similar to the neural network. However, it lacks modern computer units, such as memory, an arithmetic unit, and a controller. It is formed by combining processors with the same function [10]. An artificial neural network saves information on different unit connections. Compared with modern computers, it belongs to a completely different system that fully absorbs the advantages of a biological neural network. Its main characteristics are as follows:

(i) There are a large number of smaller processing units on the artificial neural network. The function of each unit is simple. The expected recognition effect and calculation speed determined by combining these processing units are greatly improved.

(ii) Artificial neural network has strong fault tolerance. Even if some local neurons are damaged, it will not interfere with the overall activity.

(iii) Each neuron saves all the information memorized on the neural network on the right. If one views a single right, one cannot see the information saved on it. It adopts the distributed storage mode.

(iv) The learning ability of artificial neural networks is strong. The connection structure and right on the artificial neural network can be obtained by using the learning method.

3.2. BP Neural Network Model. BP network is a multilayer feedforward neural network using the error backpropagation algorithm. Figure 1 shows the structure of the BP network. Its components include a hidden layer, input layer, and output layer. The neurons of each layer are connected with all neurons on the lower layer, and the direction of information flow is indicated by arrows [11]. In the learning process, the network is used to return information and update the connection strength. The remarkable feature of the neural network model is that no feedback is used to connect each layer of neurons. Also, there is no connection between neurons in each layer. There are only adjacent neurons connected.

The basic principle of the BP algorithm is to divide the learning process into two parts by using the idea of an error backpropagation algorithm. The first is the forward propagation process, while the second is the backpropagation process. After a group of network input values is determined, the input layer performs weighting processing and transmits them to the hidden layer. The activation function on the hidden layer processes them as the input on the output layer. After the processing by the activation function on the output layer, the corresponding network output is obtained. This process needs to be updated layer by layer as it belongs to forward propagation.

3.3. BP Neural Network Learning Algorithm. In this section, the process and structure of the BP neural network learning algorithm are explained. The explanation is as follows.

3.3.1. BP Neural Network Learning Algorithm Process. If the output vector d and the input vector x are fixed, the BP algorithm operation can be completed according to the following process:

(i) Submit information to the network input layer and obtain the y output vector in the output layer through forwarding propagation. In the process of continuing to propagate information in the network, it is necessary to clarify the sum of its input I_t and output state x_t to all neurons on the network.

(ii) Calculate the weight correction amount and local error value of all neurons on the output layer.

(iii) Accumulate the modified weights on the previous corresponding weights to effectively update each weight in the network. In the above process, the basic computer system of the BP neural network is defined. Different layers on the network are used to propagate to the output layer. The output process is where the error analysis takes place. The error is then sent through the network from the output layer to the input layer. The algorithm box is shown in Figure 2.

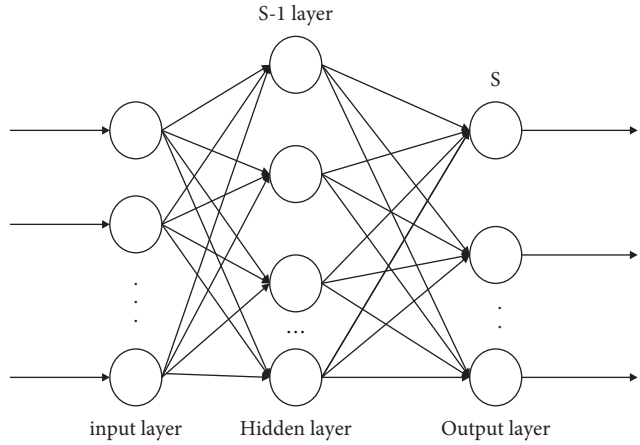

Figure 1: BP network structure diagram.

3.3.2. BP Neural Network Structure. This paper uses the backpropagation algorithm to establish the model. The structure is composed of three layers, namely, the output layer, input layer, and hidden layer. There are three nodes on each input layer and one node on the output layer. The nodes on the hidden layer are identified through the training network. In this paper, BP neural network is used to establish a model to analyze the welding direction of metal materials. The network structure is named ED-BP neural network. The inputs of different neurons in the hidden layer of the column are as follows:

$$Ii = \sum_{j=1}^{n} W_{ij} x_j, \quad (i = 1, \ldots, m;\ j = 1, 2, \ldots, n). \tag{1}$$

The following are the outputs of different neurons on the hidden layer:

$$O_t = f(I_t) = \frac{1}{1 + e^{-1}}, \quad (i = 1, \ldots\ldots, m). \tag{2}$$

The neuron output on the output layer is the network output:

$$y = \sum_{i=1}^{m} O_i V_i, \quad (i = 1, \ldots\ldots, m). \tag{3}$$

The weight connecting the input layer and the hidden layer is represented by W_{ij}. The weight connecting the hidden layer and the output layer is represented by V_t. The following is the calculation formula of sigmoid function:

$$f(x) = \frac{1}{1+e^{-x}}, \quad (0 < f(x) < 1). \tag{4}$$

Most of the constructed networks are single output and multiple input. It is assumed that the learning samples are represented by the following:

$$\left(x_{1p}, x_{2p}, \ldots, x_{np}; t_p\right), \quad (p = 1, 2, \ldots, p), \tag{5}$$

where p is the number of samples.

The network output error is represented by

$$d_p = t_p - y_p. \tag{6}$$

The error function calculated by the above formula is as follows:

$$E_p = \frac{1}{2}\left(t_p - y_p\right)^2. \tag{7}$$

Assuming that p is the learning sample, the elements in Δw are as follows:

$$\Delta V_t = \eta d_p \frac{\partial y_p}{\partial V_t} = \eta d_p f'(y_k) O_{\text{ip}} = \eta d_p O_{\text{ip}}. \tag{8}$$

Assumed input node error:

$$\delta_k = d_p f'(y_k). \tag{9}$$

Then,

$$\Delta V_I = \eta \delta_k O_{\text{ip}}. \tag{10}$$

If the hidden node error is

$$\delta_t = \delta_k V_t f'(I_t). \tag{11}$$

then

$$\Delta W_{tJ} = \eta \delta_t x_{JP}. \tag{12}$$

After iterative calculation,

$$\begin{aligned} W_{tJ}^{(n)} &= \eta \frac{\partial E_p}{\partial W_{ij}} + \alpha \Delta W_{ij}^{(n-1)}, \\ \Delta V_i^{(n)} &= -\eta \frac{\partial E_p}{\partial V_i} + \alpha \Delta V_i^{(n-1)}. \end{aligned} \tag{13}$$

Complete the forward and reverse calculations using the above method after identifying the network structure.

4. Analysis of Welding Performance of Metal Based on Neural Network

This paper studies the welding performance analysis of the metal-based neural network. The filler metals selected in various welding methods are mainly welding materials. The metallurgical operation in different stages of the welding process is realized through welding materials [12]. During manual arc welding, part of the welded metal and the electrode melt is under the action of the high heat of the arc. Under the influence of the arc blowing power, the welded metal creates a molten pool on the surface. After melting, the electrode progressively transfers to the molten pool. During the melting of the electrode coating, some liquid slag and protective gas will be generated. The generated gas will be filled near the molten pool and arc. It has the function of isolating the atmosphere. Through analysis, it is concluded that the electrode has a direct impact on the stability of the welding arc, mechanical properties, and chemical composition of the weld. Hence, it is concluded that the quality of the weld directly determines the quality of the electrode.

4.1. Analysis of Welding Chemical Composition of Metal Materials. The main function of the welding core in the welding process is that the conduction of the welding current generates a large amount of arc. The second step is to melt the welding core into the filler metal and then fuse the easily melted metal to form the weld. In the process of manual arc welding, the proportion of core metal on the weld metal reaches 50% to 70%. Hence, the performance and chemical composition of the core have a decisive impact on the weld quality. The chemical composition of common welding steel wire is listed in Table 1 (%).

In the process of metal welding, the quality of electrode will be assessed from the following three aspects:

(i) *Intrinsic Properties*: It refers to the elongation, strength, and low-temperature impact toughness.

(ii) *Appearance Quality*: It is top, eccentric, but not dried or bent.

(iii) *Welding Process Performance*: It is arc stabilization, arc striking, and slag removal.

The actual operation skills of workers and the rationality of the production process directly determine the appearance quality. However, the welding process performance is based on the components in the welding equipment, electrode coating formula, welder experience, and technology. The reasonable electrode formula directly determines the internal performance of the electrode.

4.2. Neural Network Learning Sample Collection. When analyzing the welding performance of metal based on an artificial neural network, the sample data are collected first. A sample contains a set of input and output data. In this paper, a total of 270 groups of test sample data are selected, of which 180 groups are selected to build a model to complete the training operation and build a network layer weight coefficient matrix to quickly process the sample data. 90 groups were randomly selected as a batch, and the other 90 groups tested the generalization mapping ability of the network model.

4.2.1. Collect Learning Samples. According to the above research, it is found that the content of Mn and C in welding rods directly affects the tensile strength of the metal. The

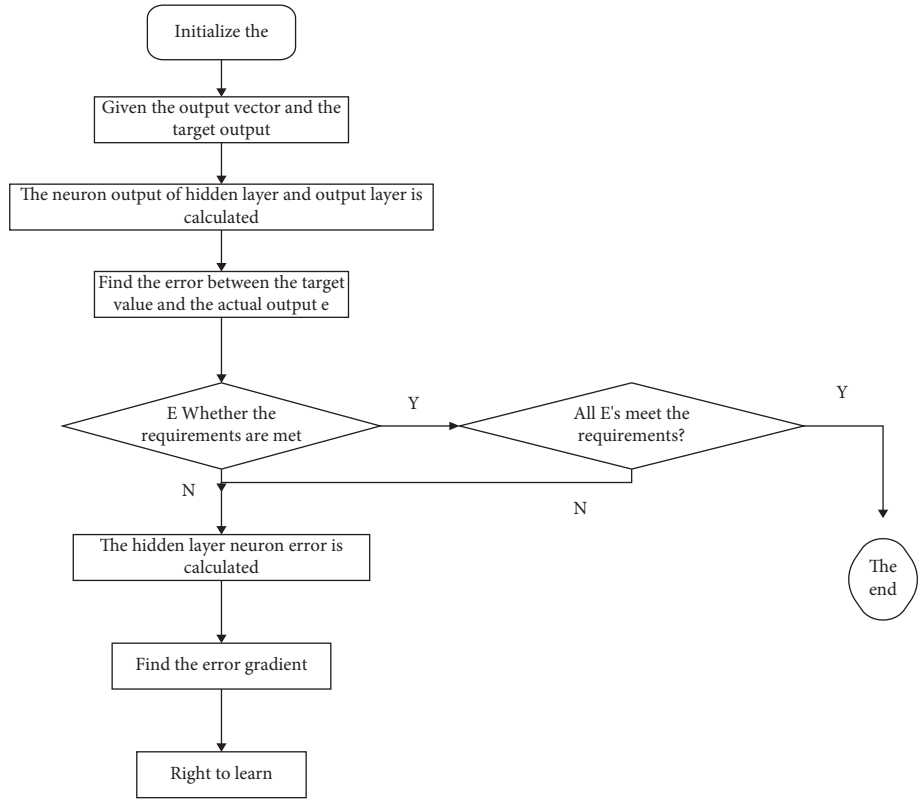

Figure 2: BP neural network algorithm process.

Table 1: Chemical composition of common welding steel wire (%).

Brand	C	Mn	Si	Cr	Ni	Cu	S	P
H08	≤0.1	0.3–0.55	≤0.03	≤0.2	≤0.3	≤0.2	≤0.04	≤0.04
H08 A	≤0.1	0.3–0.55	≤0.03	≤0.2	≤0.3	≤0.2	≤0.03	≤0.04
H08e	≤0.1	0.3–0.55	≤0.03	≤0.2	≤0.3	≤0.2	≤0.03	≤0.04

content of C in synthetic rutile, ferromanganese, and reduced pyrite should be analyzed in the total content of C in the peel component. The Mn in the flux cover and the iron-carbon-manganese in the core are transformed into Mn in the metal. The proportion of Mn in the core transition reaches 70%, and the remaining 30% is included in the transitional Mn in the iron-carbon-manganese.

$$\begin{aligned} x_1 &= C_{\text{total}}\% = 70\% \times a + 30\% \times (b + c + d), \\ x_2 &= M_{nx}\% = 70\% \times u, \\ x_3 &= M_{ny}\% = 30\% \times z. \end{aligned} \tag{14}$$

Formula a indicates the content of C in the core. Similarly, b indicates the content of C in ferromanganese and carbon in the peel; c indicates the content of C in synthetic rutile; d indicates the content of C in reduced ilmenite; u indicates the content of Mn in the core; z indicates the content of Mn in FERROCARBON and manganese. x_1 represents the total content of C in the electrode. x_2 indicates the content of Mn in the converted core. x_3 indicates the amount of Mn in the translated drug. The three inputs on the network are represented by x_1, x_2, and x_3, respectively.

4.2.2. Data Processing of Samples. An artificial neural network can only represent input data in numerical form. To code or transform external information, it is necessary to set the input information scale to a certain interval. Referring to the above formula to get the expected network output and x_1, x_2, x_3, in this paper, the sigmoid function is selected as the excitation function of neurons in the network. It can make full use of the characteristics of sigmoid function, exert the nonlinear characteristics of network neurons, and normalize the learning samples so that all data can be taken in [0,1] intervals. The following is a detailed process.

The sample data are represented by

$$x_p\,(p = 1, 2, \ldots, P). \tag{15}$$

By defining $x_{\min} = \min\{x_p\}$, $x_{\max} = \max\{x_p\}$, the normalization calculation is completed by the following formula:

$$\frac{x_p - x_{mu} + u}{x_{\max} - x_{\min} + u} \Rightarrow xp\,(0 < u < 1). \tag{16}$$

After transforming the sample data in the range of 0–1, the network input data can be normalized. The normalization of the network output data can be completed by using formula (16). The smaller number is selected as the connection right of network W. Therefore, the network will not overflow. The learning samples used in web-based learning are normalized. When using the network detection after learning, the same data should be used to transform the real data as the network input data. At the same time, the

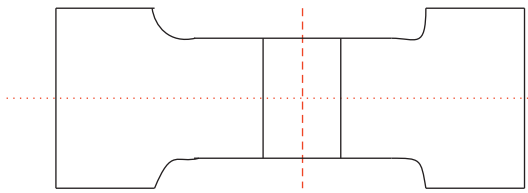

Figure 3: Tensile specimen of welded joint.

Table 2: Tensile strength test result (MPa).

Sample	The yield strength	Tensile strength	Fracture location
LTT1	467.5	539	Parent metal
LTT2	487	538	Parent metal
LTT3	517	580	Parent metal
Homogeneous	406	494	Parent metal

network output data and the restoring calculation are also calculated. The following are the restoring calculation formulas:

$$x_p\left(x_{\max} - x_{\min} + u\right) + x_{\min} - u \Rightarrow x_p. \tag{17}$$

4.3. Tensile Test. The tensile test is the most widely used method to analyze the mechanical properties of welded joints of metal materials. A large amount of data for evaluating the properties of welded joints can be calculated using the weld tensile test [13]. In this paper, WE-600 hydraulic universal testing machine is selected as the tensile test equipment. The sample size of the tensile test is determined according to the GB2651-2008 sampling standard formulated by the state for the weld tensile test. It is shown in Figure 3.

5. Welding Performance Result Analysis

In this section, the experimental results of welding tension are explained in order to analyze the tensile strength test results. It is being followed by the analysis of influencing factors of metal material welding. The explanation is as follows.

5.1. Experimental Results of Welding Tension. In this paper, the weld properties of metal materials are analyzed based on the artificial neural network. The tensile properties of metal materials are judged by tensile tests. The fracture positions of weld joints obtained by low-temperature phase-change welding wire and homogeneous weld during tensile tests are base metal. The results of tensile strength tests of metal materials are listed in Table 2. The postwelded joints of low-temperature phase-change welding wire have higher tensile strength than those filled with the same quality wire. The basic principle of equal strength matching can be observed during welding.

The tensile properties of the welded joints measured in the table above show that the strength of the weld metal is higher than the base metal. All the fracture surfaces are at the base metal in the heat-affected zone. The tensile strength of welded joints with the same filler wire composition is about 500 MPa, the yield strength is about 400 MPa, the yield strength of low-temperature phase-change welded joints is between 470 and 520 MPa, and the tensile strength is between 540 and 580 MPa. The welding process adopts the near-strong matching mode.

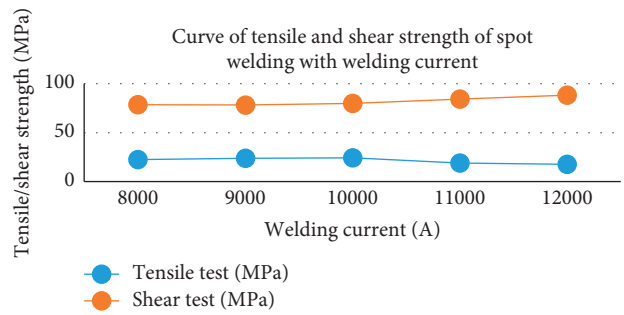

Figure 4: Change curve of tensile and shear strength of spot welding after changing welding current.

5.2. Analysis of Influencing Factors of Metal Material Welding. The main factors affecting the welding quality of metal materials are electrode pressure, welding current, and energizing time. Welding current is the nugget produced by thermal capacity during spot welding. If the welding current is small, enough heat will lack in the welding area. This will affect the strength of the spot welding. Excessive welding current causes high heat. It results in distortion of the welding area and a large number of bubbles generated by molten metal splashing. Increasing the prepressure of welding can keep the resistance of the welding area even. It is convenient to prevent local overheating. If the welding pressure is low, local heat will be too high resulting in the splashing of molten metal in the weld joint forming cracks and bubbles. Higher pressure reduces contact resistance, increases indentation, and interferes with weld strength. Another influencing factor of spot welding is power-on time. A lot of heat is wasted if the power-on time is too long. It will modify the spot welding substance. Short energizing time will result in insufficient welding and reduced weld strength.

In this paper, the shear strength and tensile strength of weld joints are tested by the shear test and tensile test. Different electrode pressures, welding current, and energizing times are set. The influence of these parameters on the tensile strength and shear strength of spot welding is analyzed [14]. Figure 4 shows the change curve of tensile and shear strength of spot welding after changing the welding current.

The welding pressure set in Figure 4 is 40 psi, i.e., 0.2758 MPa with the welding time of 0.2 seconds. The welding current rises from 8000-12000 A in order to analyze the change of tensile strength and shear strength of spot welding. According to the data in the figure, the spot welding strength increases continuously with increasing welding current. The tensile strength of spot welding increases rapidly when the welding current is higher than 10000 A and

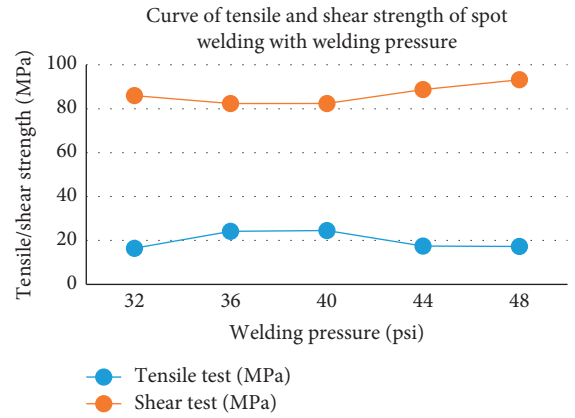

Figure 5: Tensile and shear strength curves of spot welding under varying welding pressure.

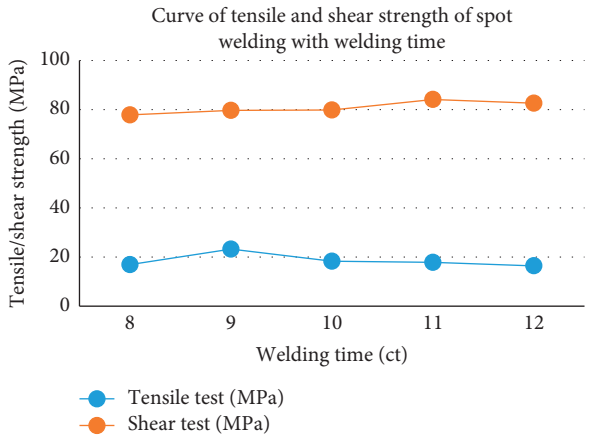

Figure 6: Curves of tensile and shear strength of spot welding with welding time.

increases slowly when the current is less than 10000 A. The shear strength of spot welding decreases rapidly from 24.25 MPa to 18.84 MPa when the spot welding current is higher than 10000 A.

The data shown in Figure 5 are 10000 A welding current and 0.2S welding time, and the welding pressure is 1psi = 0.006895 MPa. The trend of shear strength and tensile strength of spot welding is analyzed when the welding pressure increases from 32-48 psi. The welding pressure is increased from 32 psi to 40 psi, and the tensile strength is increased from 16.47 MPa to 24.52 MPa. The tensile strength continues to decrease with increasing welding pressure and decreases to 17.26 MPa at 48 psi. On the contrary, the shear strength decreases to 82.36 MPa at 40 psi welding pressure and 93.14 MPa at 48 psi welding pressure.

The influence of changing the spot welding time on tensile and shear strength is tested. The welding pressure is set at 40 psi, and the welding current is 10000 A. The corresponding change of spot welding tensile and shear strength is shown in Figure 6, and 1 CT is equal to 0.02s. Analysis of the above-broken line diagram shows that the tensile and shear strengths reach the highest when welding time is 11 CT, 17.78 MPa, and 84.12 MPa, respectively. Overall, the tensile and shear strengths increase and decrease first with the prolongation of welding time.

6. Conclusions

Artificial neural networks are strong tools for analysis, modeling, and control applications, according to the tests and research conducted for this study. They are especially appealing because of their ability to interpret nonlinear and noisy input, learn from actual welding data, and execute at a fast rate. All of the topics investigated in this study appear to have a lot of promise for practical applications. However, it has a little application in metal material welding. Only a few scholars have studied it. Based on the advantages of artificial intelligence technology, this paper makes full use of the characteristics of this algorithm in the analysis of the welding performance of metal materials. Through in-depth analysis of the calculation process and the basic structure of artificial intelligence algorithm, it builds an artificial algorithm model which uses shear test and tensile test methods to test shear strength and tensile strength of welded joints by setting different welding times and welding pressure. The test results show that the tensile strength increases continuously with the increase of welding current. When the welding current is 10000A, the shear strength of spot welding decreases rapidly from 24.25 MPa to 18.84 MPa. Similarly, tensile strength and shear strength increase and decrease at first when prolonging welding time. When the welding pressure changes in the range of 32 psi-48 psi, the tensile strength increases from 16.47 MPa to 24.52 MPa and then decreases to 17.26 MPa. The shear strength is the opposite, decreasing first and then decreasing again [15–20].

Data Availability

The data used to support the findings of the study are included within the article.

Conflicts of Interest

The author declares that there are no conflicts of interest.

References

[1] V. N. Arisova, L. M. Gurevich, A. F. Trudov, A. G. Serov, and V. G. Kharlamov, "Structure formation in the zones of joints obtained by explosion welding with subsequent rolling of a five-layer titanium-steel composite," *Metallurgist*, vol. 63, no. 1-2, pp. 96–104, 2019.

[2] J. Reimann, P. Henckell, Y. Ali et al., "Production of topology-optimised structural nodes using arc-based, additive manufacturing with GMAW welding process," *Journal of Civil Engineering and Construction*, vol. 10, no. 2, pp. 101–107, 2021.

[3] K. Mahmud, S. P. Murugan, Y. Cho, C. Ji, D. Nam, and Y.-D. Park, "Geometrical degradation of electrode and liquid metal embrittlement cracking in resistance spot welding," *Journal of Manufacturing Processes*, vol. 61, pp. 334–348, 2021.

[4] I. I. Tagiltsev and A. V. Shutov, "Assessment of residual stresses in a T-joint weld by combined experimental/

theoretical approach," *Journal of Physics: Conference Series*, vol. 1945, no. 1, Article ID 012059, 2021.

[5] C. V. Govindan, D. Jeyasimman, and M. Ganesh, "Detection defects surface of welding image with transform coefficients," *Solid State Technology*, vol. 63, no. 3, pp. 4106–4119, 2020.

[6] P. Leo, G. Renna, G. Casalino, and A. G. Olabi, "Effect of power distribution on the weld quality during hybrid laser welding of an Al-Mg alloy," *Optics & Laser Technology*, vol. 73, pp. 118–126, 2015.

[7] J. Ren, Z. Li, N. Jia, C. Liu, and T. Xue, *Wire-feeding Speed Measurement System Based on Hall Sensor*, Electric Welding Machine, Mahindra World City, 2018.

[8] T. A. Nguyen, H. B. Ly, H. V. T. Mai, and V. Q. Tran, "Using ANN to Estimate the Critical Buckling Load of Y Shaped Cross-Section Steel Columns," *Scientific Programming*, vol. 2021, Article ID 5530702, 2021.

[9] A. S. Chaus, A. Kuhajdová, M. Marônek, and M. Dománková, "Effect of multiple local repairs on microstructure and mechanical properties of T24 steel welded joint," *Journal of Materials Engineering and Performance*, vol. 27, no. 6, pp. 3024–3034, 2018.

[10] J. Lin, Y. Zhang, T. Zhao, and Y. Su, "Structure strength assessment method of distribution network based on improved convolution neural network and network topology feature mining," *Proceedings of the CSEE*, vol. 39, no. 01, pp. 86–98, 2019.

[11] G. S. Kumar, M. Ramesh, S. Dinesh, P. Paramasivam, and N. Parthipan, "Investigation of the TIG welding process for joining AA6082 alloy using grey relational analysis," *Advances in Materials Science and Engineering*, vol. 2022, pp. 1–8, Article ID 5670172, 2022.

[12] L. Leif, "Welding duplex stainless steels - a review of current recommendations," *Welding in the World*, vol. 56, no. 5-6, pp. 65–76, 2012.

[13] J. Guo, P. Gougeon, and X.-G. Chen, "Microstructure evolution and mechanical properties of dissimilar friction stir welded joints between AA1100-B4C MMC and AA6063 alloy," *Materials Science and Engineering A*, vol. 553, pp. 149–156, 2012.

[14] Y. Ma, B. Yang, M. Lou, Y. Li, and N. Ma, "Effect of mechanical and solid-state joining characteristics on tensile-shear performance of friction self-piercing riveted aluminum alloy AA7075-T6 joints," *Journal of Materials Processing Technology*, vol. 278, Article ID 116543, 2020.

[15] S. Kumar, A. S. Shahi, V. Sharma, and D. Malhotra, "Effect of welding heat input and post-weld thermal aging on the sensitization and pitting corrosion behavior of AISI 304L stainless steel butt welds," *Journal of Materials Engineering and Performance*, vol. 30, no. 3, pp. 1619–1640, 2021.

[16] Z. S. Al Sarraf, A. F. Ahmed, and K. A. Hamoo, "Evaluation of vibration amplitude stepping and welding performance of 20 kHz and 40 kHz ultrasonic power of metal welding," *Journal of Mechanical Engineering Research*, vol. 4, no. 1, 2021.

[17] A. Chiocca, F. Frendo, and L. Bertini, "Evaluation of residual stresses in a pipe-to-plate welded joint by means of uncoupled thermal-structural simulation and experimental tests," *International Journal of Mechanical Sciences*, vol. 199, Article ID 106401, 2021.

[18] N. Akkas, D. Karayel, S. S. Ozkan, A. Oğur, and B. Topal, "Modeling and analysis of the weld bead geometry in submerged arc welding by using adaptive neurofuzzy inference system," *Mathematical Problems in Engineering*, vol. 2013, pp. 1–10, Article ID 473495, 2013.

[19] R. Saha and P. Biswas, "Temperature and stress evaluation during friction stir welding of inconel 718 alloy using finite element numerical simulation," *Journal of Materials Engineering and Performance*, vol. 31, no. 3, pp. 2002–2011, 2021.

[20] R. K. Aggarwal, M. M. Mourelle, S. Kristoffersen et al., "Development and qualification of alternative solutions for improved fatigue performance of deepwater steel catenary risers," *International Conference on Offshore Mechanics And Arctic Engineering*, vol. 42673, pp. 315–329, 2007.